Fast Multi-Satellite ML Acquisition for A-GPS

Seung-Hyun Kong, *Member, IEEE*

***Abstract*—Successful position fix in harsh environments such as indoors and dense urban canyons is a strongly required capability for an assisted global positioning system (A-GPS) receiver. In recently developed cellular networks, receiving fine time assistance and maintaining high-frequency accuracy using downlink measurements are not possible for A-GPS receivers, since node-Bs are asynchronous and are not equipped with a source for precise time and frequency. In this paper, we propose a correlator-based fast multi-satellite maximum likelihood (MSML) algorithm, for A-GPS receivers in asynchronous networks, that achieves fast acquisition utilizing fast computation techniques. From numerous Monte Carlo simulations, it is demonstrated that the proposed fast MSML algorithm, when compared with conventional correlator-based acquisition techniques used in standalone GPS and A-GPS receivers, provides higher detection sensitivity for weak signals in the presence of other strong signals by removing strong inter-satellite interference (ISI).**

***Index Terms*—Assisted global positioning system (A-GPS), asynchronous cellular network, multi-satellite maximum likelihood (MSML).**

I. Introduction

ASSISTED Global Positioning System (A-GPS) has been the enabler of many mobile location-based services (LBS) and is the most popular mobile location technology in recent years. Using acquisition and sensitivity assistance from cellular networks [1] and [2], an A-GPS receiver can achieve a faster signal acquisition and higher detection sensitivity than standalone GPS receivers. The acquisition assistance conveys information about the prompt code phase (i.e., fine timing) and precise Doppler frequency of GPS signals measured by the nearest base station so that an A-GPS receiver in the coverage area of the base station can significantly reduce the size of two-dimensional (code phase and Doppler frequency) search space. For example, in synchronized networks such as IS-95 and CDMA2000, the clock and frequency source to generate downlink channels is a GPS-synchronized oscillator in the base station so that the downlink signal can provide a fine time reference with microseconds of uncertainty [1] as well as a precise frequency reference to an A-GPS receiver. However, in asynchronous networks, such as Global System for Mobile (GSM) [3], 3rd Generation Wideband Code Division Multiple Access (3G WCDMA) [4], and 4G Long Term Evolution (LTE) [5], node-Bs are not using GPS so that the timing and frequency accuracy of downlink signals are not very reliable for A-GPS receivers. In addition, due to internal processing errors, clock and frequency signals generated from downlink measurements by a user equipment (UE) can be as poor as ± 0.2 ppm [6].

There have been a number of GPS signal search techniques introduced in the literature [7]–[12], and the search techniques utilize auto-correlation between the incoming signal and a receiver replica signal. Among serial search techniques, double or multiple dwell serial search techniques have become a popular choice to reduce mean acquisition time (MAT) [8], and the Two-Dimensional Compressed Correlator (TDCC) technique [9] is one of the recent techniques achieving a small MAT. Due to the evolution of electronics, parallel search techniques using frequency domain multiplications can be efficiently implemented in a cheap DSP (Digital Signal Processor) [7], [10]–[12]. The (dual) folding technique [13] and [14] is introduced recently to quickly acquire an incoming GPS signal. However, these auto-correlation-based search techniques often suffer from inter-satellite interference (ISI), when a target GPS signal to detect is much weaker than other incoming GPS signals. In practice, strong ISI occurs very often in harsh GPS environments, since GPS signals are designed to have similar power levels when arriving at a ground receiver in open sky environments.

There have been a few studies on the simultaneous acquisition of multi-satellites (MS) to improve the detection sensitivity for weak GPS signals introduced in the literature. In [15], a maximum likelihood (ML) multi-satellite acquisition algorithm similar to the ML direction finding algorithm for array antenna systems is introduced. The ML algorithm in [15] searches all the possible code phase and Doppler frequency hypotheses with a fine resolution and shows significant SNR improvement in detecting weak GPS signals in the presence of stronger GPS signals, but the algorithm is computationally expensive. In [16], a coherent MS acquisition technique is proposed for an A-GPS system in a synchronous cellular network, where it is assumed that a synchronized node-B can provide UE fine timing and frequency reference as well as the precise carrier phase measurements of all GPS satellites in view. The algorithm in [16] is not useful to the asynchronous cellular networks and also requires a huge computational cost. In [17], simultaneous non-coherent MS acquisition technique that is applicable to A-GPS in a synchronous cellular network is introduced. In most previous studies on coherent MS acquisition algorithm and ML algorithm, computational complexity has been a major drawback. However, there has been little studies so far to reduce

Manuscript received July 28, 2013; revised January 20, 2014 and May 7, 2014; accepted May 23, 2014. Date of publication May 29, 2014; date of current version September 8, 2014. This work was supported by a grant from Development of GNSS-Based Transportation Infrastructure Technology funded by the Ministry of Land, Transport, and Maritime Affairs of the Korean government. The associate editor coordinating the review of this paper and approving it for publication was A. Giorgetti.

The author is with the CCS Graduate School for Green Transportation, Korea Advanced Institute of Science and Technology, Daejeon 305-701, Korea (e-mail: skong@kaist.ac.kr).

Color versions of one or more of the figures in this paper are available online at http://ieeexplore.ieee.org.

Digital Object Identifier 10.1109/TWC.2014.2327101

the computational complexity required for the MS acquisition algorithms and MS-ML (or MSML in short) algorithms, and no MS or MSML algorithm has been investigated for an application to the A-GPS system, in asynchronous cellular networks, where a simple single-satellite (satellite by satellite) acquisition technique is implemented currently [18].

In this paper, we propose a fast MSML acquisition algorithm applicable to A-GPS receivers in asynchronous cellular networks. The proposed fast MSML algorithm is different from the MSML algorithm in [15] in that the proposed fast MSML algorithm is computationally efficient as it employs three fast computation algorithms proposed in this paper while implementable with correlators. The three fast computation techniques are algebraic approximation of cross-correlations, deterministic estimation of signal amplitudes and carrier phases, and search space reduction utilizing relative code phase and Doppler frequency hypotheses for A-GPS in asynchronous cellular network. We provide theoretical analysis and performance comparison to the conventional correlator-based acquisition techniques using numerous Monte Carlo simulations. The remainder of this paper is organized as follows. Mathematical models of the MSML estimation are derived in Section II, and techniques to reduce mathematical computations for the MSML estimation in Section II is introduced in Section III. Theoretical performance analysis are provided in Section IV and simulation results for the performance and complexity comparison to other similar techniques are introduced in Section V. The conclusion is in Section VI.

II. MSML Estimator

Let $r_{RF}(t)$ be the incoming L1 frequency GPS coarse acquisition (C/A) code signals received by an A-GPS receiver located at an unknown horizontal location (x, y) connected to an asynchronous node-B at the origin (0,0). When $r_{RF}(t)$ is frequency down converted to an IF frequency f_{IF}, the real valued received IF signal can be expressed as

$$r(t) = \sum_{k=1}^{K} a_k d_k(t-\lambda_k) c_k(t-\lambda_k) \cdot \cos\left(2\pi\left(f_{IF}+f_D^k\right)t+\phi_k\right)+n(t), \quad (1)$$

where K is the number of GPS satellite signals being received, a_k, λ_k, f_D^k, and ϕ_k are the slowly varying amplitude, propagation delay, Doppler frequency, and unknown carrier phase of the kth satellite signal, respectively, $d_k(t)$ and $c_k(t)$ are the navigation data bit and pseudo-random noise (PRN) code of the kth satellite at time t, respectively, and $n(t)$ represents an additive white Gaussian noise (AWGN) with two-sided power spectral density (PSD) $N_0/2$. In this paper, it is assumed that $|f_D^k| \le 5$ kHz. Let $s_k(t)$ represent the incoming signal of GPS satellite k estimated by the A-GPS receiver such that

$$s_k(t) = \hat{a}_k c_k(t-\hat{\lambda}_k)\cos\left(2\pi\left(f_{IF}+\hat{f}_D^k\right)t+\hat{\phi}_k\right), \quad (2)$$

where

$$S_k = \left\{\hat{a}_k, \hat{\lambda}_k, \hat{f}_D^k, \hat{\phi}_k\right\} \quad (3)$$

is the set of parameters to be estimated for the satellite k, and $\hat{a}_k$, $\hat{\lambda}_k$, $\hat{f}_D^k$, and $\hat{\phi}_k$ are the estimated signal amplitude, propagation delay, Doppler frequency, and carrier phase of the satellite k, respectively, by the receiver. Using (1) and (2), the MSML estimation can be modeled as

$$\hat{S} = \arg\max_S \exp\left(-\frac{\left[r(t)-\sum_{k=1}^{K} s_k(t)\right]^2}{N_0}\right)$$

$$= \arg\max_S \left(2r(t)\sum_{k=1}^{K} s_k(t) - \left[\sum_{k=1}^{K} s_k(t)\right]^2\right), \quad (4a)$$

$$= \arg\max_S \left(2\int_0^T r(t)\sum_{k=1}^{K} s_k(t)\,dt - \int_0^T \left[\sum_{k=1}^{K} s_k(t)\right]^2 dt\right) \quad (4b)$$

$$= \arg\max_S (2L_{AC} - L_{CC}), \quad (4c)$$

where

$$S = \{S_k | k = 1, 2, \ldots, K\}, \quad (5)$$

$\hat{S}$ is the solution of the MSML estimator, (4a) can be obtained, since $\exp(\cdot)$ is a monotonically increasing function, and the MSML estimator in (4b) is an expression realizable with correlators. The first integration in (4b), denoted as L_{AC} in (4c), shows the auto-correlation between the incoming signal $r(t)$ and the sum of the receiver replica signal $s_k(t)$, the second integration in (4b), denoted as L_{CC} in (4c), represents ISI, and T is the integration interval that is assumed to be much smaller than a bit interval T_b (=20 ms). Note that the MSML estimator (4c) actually removes the ISI by canceling out the cross-correaltions L_{CC} from the auto-correlation results L_{AC}. Note also that there are K auto-correlations to produce L_{AC} and obtaining L_{CC} requires $K(K-1)/2$ cross-correlations so that $K(K+1)/2$ correlations are needed to be done for every different set of parameters S, which may be too much computational complexity for a cheap A-GPS receiver.

In the following analysis, we assume that $d_k(t-\lambda_k)(=\pm 1)$ is constant during the short interval $T(\ll T_b)$ for $K(\le 10)$ visible satellites, and that the effect of $d_k(t-\lambda_k)$ can be included in the unknown carrier phase ϕ_k. In addition, since $c(t)$ is T_1-periodic ($T_1 = 1$ ms), we can substitute λ_k with τ_k in (1) and (2) and assume that $0 \le \tau_k \le 1$ ms and $0 \le \hat{\tau}_k \le 1$ ms represent the code phase and the estimated code phase of the incoming signal of satellite k in seconds, respectively. Defining

$$\alpha_k^I = \hat{a}_k \cos(\hat{\phi}_k) \quad (6a)$$

$$\alpha_k^Q = \hat{a}_k \sin(\hat{\phi}_k) \quad (6b)$$

$$c_k^I(t) = c_k(t-\hat{\tau}_k)\cos\left(2\pi\left(f_{IF}+\hat{f}_D^k\right)t\right) \quad (6c)$$

$$c_k^Q(t) = c_k(t-\hat{\tau}_k)\sin\left(2\pi\left(f_{IF}+\hat{f}_D^k\right)t\right), \quad (6d)$$

$s_k(t)$ can be expressed as

$$s_k(t) = \alpha_k^I c_k^I(t) - \alpha_k^Q c_k^Q(t). \quad (7)$$

respectively. Using (7), L_{AC} can be expressed as

$$L_{AC} = \sum_{k=1}^{K} \alpha_k^I R_k^I - \alpha_k^Q R_k^Q, \tag{8}$$

where

$$R_k^I = \mathrm{Re}\{R_k\} = \mathrm{Re}\left\{ \int_0^T r(t) \left(c_k^I(t) + j c_k^Q(t) \right) dt \right\} \tag{9a}$$

$$R_k^Q = \mathrm{Im}\{R_k\} = \int_0^T r(t) c_k^Q(t)\, dt, \tag{9b}$$

and L_{CC} can be expressed as

$$\begin{aligned} L_{CC} &= \int_0^T \sum_{k=1}^{K} \sum_{m=1}^{K} \left(\alpha_k^I c_k^I(t) - \alpha_k^Q c_k^Q(t) \right) \\ &\quad \times \left(\alpha_m^I c_m^I(t) - \alpha_m^Q c_m^Q(t) \right) dt \\ &= \sum_{k=1}^{K} \sum_{m=1}^{K} \left[\alpha_k^I \alpha_m^I \int_0^T c_k^I(t) c_m^I(t)\, dt \right. \\ &\qquad + \alpha_k^Q \alpha_m^Q \int_0^T c_k^Q(t) c_m^Q(t)\, dt \\ &\qquad - \alpha_k^I \alpha_m^Q \int_0^T c_k^I(t) c_m^Q(t)\, dt \\ &\qquad \left. - \alpha_k^Q \alpha_m^I \int_0^T c_k^Q(t) c_m^I(t)\, dt \right]. \end{aligned} \tag{10}$$

Since a multiplication of two sinusoidal signals of frequency $f_{IF} + f_D^k$ and $f_{IF} + f_D^m$ is a sum of two sinusoidal signals of frequencies $2f_{IF} + f_D^k + f_D^m$ and $f_D^k - f_D^m$ (low frequency term), L_{CC} can be approximated by the low frequency term as

$$\begin{aligned} L_{CC} &\simeq \sum_{k=1}^{K} \sum_{m=1}^{K} \int_0^T c_k(t - \hat{\tau}_k) c_m(t - \hat{\tau}_m) \\ &\quad \times \left[\frac{\left(\alpha_k^I \alpha_m^I + \alpha_k^Q \alpha_m^Q \right)}{2} \cos\left(2\pi \left(f_D^k - f_D^m \right) t \right) \right. \\ &\qquad \left. + \frac{\left(\alpha_k^I \alpha_m^Q - \alpha_k^Q \alpha_m^I \right)}{2} \sin\left(2\pi \left(f_D^k - f_D^m \right) t \right) dt \right]. \end{aligned} \tag{11}$$

III. Proposed Three Computation Algorithms for a Fast MSML Estimation

In this section, we propose a fast MSML algorithm that is composed of three computationally efficient algorithms to reduce the computational complexity of the MSML estimation problem in (8) and (11). In the following three subsections, the three fast computation algorithms, fast search for $\{\tau_k, f_D^k\}$, algebraic determination of α_k, and approximated cross-correlations using pre-calculated and stored data, are introduced.

A. Reduced Search Algorithm for τ_k, f_D^k

As shown in (8) and (11), the MSML estimation (4c) requires the auto-correlations of all GPS signals and the cross-correlations between every pair of GPS signals in the received signal $r(t)$. To obtain the auto-correlations, a receiver needs to perform hypothesis testing over a 2-dimensional search space for each GPS signal, which requires a huge amount of computation and hardware resources in the receiver. Similarly, the cross-correlations require the knowledge of relative Doppler frequencies between every pair of GPS signals.

In an A-GPS system connected to an asynchronous cellular network, a remote receiver may utilize the observed code phases and Doppler frequencies of GPS signals made by a nearby node-B. In practice, a node-B in 3G or 4G is not synchronized to GPS so that the instantaneous code phase observation is not valid when it is delivered to the receiver. However, the code phase difference and the Doppler frequency difference between any pair of GPS signals are changing slowly and the measurements made by the remote receiver and the nearby node-B are very similar, since they are located relatively very closely. In this subsection, we provide justifications of utilizing the code phase difference and the Doppler frequency difference observed by the node-B for the MSML estimation in a remote A-GPS receiver.

Since an asynchronous node-B can have large clock and frequency uncertainties, the accurate time, $t = t_0$, when the prompt code phase and Doppler frequency are measured is unknown. Therefore, the measurements and the time-tag made by the node-B are not useful to predict the exact code phase and the Doppler frequency of the same GPS signal arriving at the remote A-GPS receiver in a near future time $t = t_1 = t_0 + \delta t$. However, since the clock rate of the node-B can be assumed to be constant over a short time interval δt, and the maximum code phase drift due to the satellite motion is only 3 chips per second [19], the measurements of the code phase difference between satellites k and m obtained at $t = t_0$ and $t = t_1$ by the node-B (denoted as $\delta\tau_{k,m}^B(t_0)$ and $\delta\tau_{k,m}^B(t_1)$, respectively) are approximately the same as

$$\delta\tau_{k,m}^B(t_0) \simeq \delta\tau_{k,m}^B(t_1), \tag{12}$$

where the superscript B is for a measurement by the node-B, and t_i $(i = 0 \text{ or } 1)$ denotes the time-tag of the measurement. And we can expect that the A-GPS receiver located at the same location to the node-B have

$$\delta\tau_{k,m}^A(t_1)|_{H_L(B)} = \delta\tau_{k,m}^B(t_1), \tag{13}$$

where the superscript A is for a measurement by the A-GPS receiver, and $H_L(B)$ represents the location hypothesis of node-B. Similarly to (12) and (13), since the frequency drift of the node-B can be assumed to be constant over δt, and the

maximum Doppler frequency drift due to the satellite motion is negligible (less than 1 Hz per second [19]),

$$\delta f^{B}_{k,m}(t_0) \simeq f^{k,B}_{D}\Big|_{t_1} - f^{m,B}_{D}\Big|_{t_1} \tag{14a}$$

$$\simeq \delta f^{A}_{k,m}(t_1)|_{H_L(B)}. \tag{14b}$$

In 3G WCDMA [4] and 4G LTE [5], the length of a downlink data frame is only 10 ms, and assistance data generated at $t = t_0$ by a node-B can be delivered to an A-GPS receiver within the node-B's service area in less than a few frames. Including the air propagation delay, the assistance data should arrive at the A-GPS receiver by $t = t_1 = t_0 + \delta t$, where $\delta t \ll 0.33$ s.

In practice, $\delta\tau^{A}_{k,m}(t_1)$ (13) and $\delta f^{A}_{k,m}(t_1)$ (14b) can be different from $\delta\tau^{B}_{k,m}(t_0)$ (12) and $\delta f^{B}_{k,m}(t_0)$ (14a), respectively, depending on the distance between the A-GPS receiver and the node-B. However, since Doppler frequency measurements of a satellite signal at two different locations of 1 Km apart is less than 1 Hz [19], and the radius R of a 3G or 4G node-B (sector) is usually less than a few Km,

$$\delta f^{A}_{k,m}(t_1) \simeq \delta f^{B}_{k,m}(t_1) + \delta f_e \simeq \delta f^{B}_{k,m}(t_1) \simeq \delta f^{B}_{k,m}(t_0) \tag{15}$$

for a very small δt, where δf_e is the maximum relative Doppler frequency difference between the node-B and the A-GPS receiver for any two visible satellites so that $\delta f_e \leq 10$ Hz can be assumed. However, in 3G WCDMA and 4G LTE, UE can have oscillator frequency drift up to ± 0.2 ppm [6] which can result in a maximum UE frequency offset $\max[f^{A}_{e}] = \pm 350$ Hz in practice, and

$$f^{k,A}_{D}(t_1) = f^{k,B}_{D}(t_1) + f^{A}_{e} \simeq f^{k,B}_{D}(t_0) + f^{A}_{e}. \tag{16}$$

Note that the frequency offset of the node-B when $f^{k,B}_{D}(t_0)$ was obtained is already counted in the frequency offset of the A-GPS receiver f^{A}_{e} in (16), since the A-GPS receiver relies on the observed frequency of downlink signals to tune and stabilize its internal oscillator [6]. Let Δf_m be the Doppler frequency search step size and, in this paper, we assume that $\Delta f_m = 1/(2T)$ as one of the common choices for GPS receivers [12]. Therefore, the number of Doppler frequency hypotheses $D_f = 21$ for $T = 1$ ms. Since $\Delta f_m/2 \leq \max[f^{A}_{e}] < \Delta f_m$, the A-GPS receiver needs to test at least $N_{H_f}(= 3)$ Doppler frequency hypotheses as

$$f^{m,A}_{D}(t_1) = \begin{cases} f^{m,B}_{D}(t_0) - \Delta f \\ f^{m,B}_{D}(t_0) \\ f^{m,B}_{D}(t_0) + \Delta f \end{cases} \tag{17}$$

to detect satellite m signal, where $\Delta f \leq \Delta f_m$. In addition, since the Doppler frequency of satellite k is

$$f^{k,A}_{D}(t_1) \simeq f^{m,A}_{D}(t_1) + \delta f^{A}_{k,m}(t_1) + f^{A}_{e} \simeq f^{m,A}_{D}(t_1) + \delta f^{B}_{k,m}(t_0), \tag{18}$$

the A-GPS receiver needs to test at least three Doppler frequency hypotheses for any satellite k.

Fig. 1 illustrates an example to describe the difference between $\delta\tau^{B}_{k,m}(t_1)$ and $\delta\tau^{A}_{k,m}(t_1)$ for a node-B at $H_L(B) = (0,0,0)$ and an A-GPS receiver at $(x,y,0)$ in the xyz-coordinate system. For algebraic simplicity, we assume the node-B and the A-GPS receiver are on the horizontal plane. There are two GPS satellites (k and m) at $X_k = [x_k, y_k, z_k]$ and $X_m = [x_m, y_m, z_m]$, and let their elevation and azimuth angles seen at the node-B be (E_k, A_k) and (E_m, A_m), respectively. The distance to the two satellites from the node-B and the A-GPS receiver are (l_k, l_m) and (l'_k, l'_m), respectively. Using the linear approximation in [20], the pseudorange difference at the A-GPS receiver is

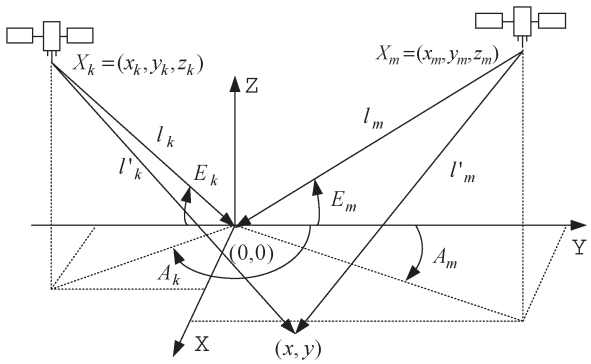

Fig. 1. An example of the relative pseudo-range.

$$\begin{aligned}(l'_k - l'_m)\,|_{t_1} &\simeq l_k - \frac{2x_k x + 2y_k y - x^2 - y^2}{l_k} \\ &\quad - l_m + \frac{2x_m x + 2y_m y - x^2 - y^2}{l_m} \\ &\simeq (l_k - l_m)|_{t_1} + 2\left(\frac{x_m}{l_m} - \frac{x_k}{l_k}\right)x + 2\left(\frac{y_m}{l_m} - \frac{y_k}{l_k}\right)y.\end{aligned} \tag{19}$$

Note that $l_k - l_m$ is related to the relative code phase difference $\delta\tau^{B}_{k,m}(t_1)$, and that the coefficients of x and y in (19) can be determined using the measurements by the node-B at $t = t_1$ and are not varying significantly during δt. From (12) and (19),

$$\delta\tau^{A}_{k,m}(t_1) \simeq \delta\tau^{B}_{k,m}(t_1) + t^{k}_{C}(x,y) \simeq \delta\tau^{B}_{k,m}(t_0) + t^{k}_{C}(x,y), \tag{20}$$

where

$$t^{k}_{C}(x,y) = \frac{1}{c}\,\mathrm{mod}\left[2\left(\frac{x_m}{l_m} - \frac{x_k}{l_k}\right)x + 2\left(\frac{y_m}{l_m} - \frac{y_k}{l_k}\right)y, cT_1\right] \tag{21}$$

for any location (x,y) within the coverage area of the node-B C, and c is the speed of light ($= 3 \times 10^8$ m/s), $T_1 = 1$ ms, and $\mathrm{mod}(a,b)$ represents a modulo b operation. Therefore, the code phase difference between the satellite k and satellite m measured by the A-GPS receiver is directly related to the assistance information such as $\delta\tau^{B}_{k,m}(t_0)$, X_m, X_k, $H_L(B)$, and the location (x,y). Using (20), the instantaneous relative code phase of the (target) satellite k to the satellite m is

$$\tau^{A}_{k}(t_1) = \tau^{A}_{m}(t_1) + \delta\tau^{A}_{k,m}(t_1) \simeq \tau^{A}_{m}(t_1) + \delta\tau^{B}_{k,m}(t_0) + t^{k}_{C}(x,y) \tag{22a}$$

$$\simeq \tau^{B}_{m}(t_0) + \delta\tau^{B}_{k,m}(t_0) + t^{k}_{C'}(x,y), \tag{22b}$$

where (22b) can be obtained from (22a) either when E_m is very large (i.e., $E_m \approx 90^\circ$) and δt very small or when C' has sufficiently wider area than C to compensate for the difference $\tau_m^B(t_0) - \tau_m^B(t_1)$. In practice, satellite m can be the one whose elevation angle is the closest to the zenith, but E_m can be slightly smaller than 90° and $\tau_k^A(t_1)$ can be a couple of chip (T_c) different from (22b). However, when C is defined for a wide enough area (of radius a few Km), we can assume $C' \simeq C$ in (22b). Therefore, denoting R as the radius of the coverage area C of the node-B, when the A-GPS receiver is provided the assistance information

$$I_{\tau_m} = \left\{\delta\tau_{k,m}^B(t_0), \tau_m^B(t_0), X_m, X_k, H_L(B), R\right\}, \tag{23}$$

the A-GPS receiver in C can find the window of possible relative code phase of the satellite k to the satellite m as

$$g_{k,m}^-(t_0) \lesssim \tau_k^A(t_1) \lesssim g_{k,m}^+(t_0), \tag{24}$$

where

$$g_{k,m}^\pm(t_0) = \tau_m^B(t_0) + \delta\tau_{k,m}^B(t_0) \pm \max\left[\left|t_{C'}^k(x,y)\right|\right]. \tag{25}$$

Therefore, there are

$$N_{H_c}(k) = \left\lceil \frac{2\max\left[\left|t_{C'}^k(x,y)\right|\right]}{\Delta t} + 1 \right\rceil \tag{26}$$

code phases to test for the satellite k, where $\Delta t\ (= 0.5T_c)$ is the code phase search step size in seconds. When the A-GPS receiver is located at the boundary of the coverage area, and the A-GPS receiver and the satellite k lie at the same azimuth angle A_k from the node-B, the relative propagation distance of the satellite k signal arriving at the node-B to that arriving at the A-GPS receiver is $R\cos(E_k)$, and

$$\frac{\max\left[\left|t_{C'}^k(x,y)\right|\right]}{\Delta t} = \frac{R\cos(E_k)}{c\Delta t}. \tag{27}$$

The proposed fast MSML algorithm can exploit FFT-based correlations to quickly obtain the auto-correlations R_k^I (9a) and R_k^Q (9b) for all $k \in \{1, 2, \ldots, K\}$ and to compute L_{AC} (8) as

$$L_{AC} = \sum_{k=1}^{K} \alpha_k^I R_k^I\left(\hat{\tau}_k^A(t_1)\right) - \alpha_k^Q R_k^Q\left(\hat{\tau}_k^A(t_1)\right), \tag{28}$$

where $\hat{\tau}_k^A(t_1)$ is one of the $N_{H_c}(k)$ possible code phases of the satellite k (24).

B. Deterministic Algorithm for α_k

In this subsection, we develop an algebraic solution to deterministically estimate the complex signal amplitudes α_k for $k = \{1, 2, \ldots, K\}$ at once. For a given set of code phase and Doppler frequency hypotheses of all K satellites, the real coefficients α_k^I (6a) and α_k^Q (6b) for the MSML (4c) can be found by taking partial derivatives of $2L_{AC} - L_{CC}$ with respect to α_k^I and α_k^Q, and set the results equal to zero as

$$\frac{\partial(2L_{AC} - L_{CC})}{\partial\alpha_k^I} = 0 \tag{29a}$$

$$\frac{\partial(2L_{AC} - L_{CC})}{\partial\alpha_k^Q} = 0. \tag{29b}$$

After some algebraic manipulations, (29a) and (29b) result in

$$\begin{aligned} R_k^I &\simeq \sum_{m=1}^{K} \int_0^T c_k(t-\hat{\tau}_k)c_m(t-\hat{\tau}_m) \\ &\quad \times \left[\alpha_m^I \cos\left(2\pi\delta f_{k,m}^A t\right) + \alpha_m^Q \sin\left(2\pi\delta f_{k,m}^A t\right)\right] dt \\ &\simeq \sum_{m=1}^{K} R_{k,m}^c \alpha_m^I + \sum_{m=1}^{K} R_{k,m}^s \alpha_m^Q \end{aligned} \tag{30a}$$

$$\begin{aligned} R_k^Q &\simeq \sum_{m=1}^{K} \int_0^T c_k(t-\hat{\tau}_k)c_m(t-\hat{\tau}_m) \\ &\quad \times \left[\alpha_m^Q \cos\left(2\pi\delta f_{k,m}^A t\right) - \alpha_m^I \sin\left(2\pi\delta f_{k,m}^A t\right)\right] dt \\ &\simeq \sum_{m=1}^{K} R_{k,m}^c \alpha_m^Q - \sum_{m=1}^{K} R_{k,m}^s \alpha_m^I, \end{aligned} \tag{30b}$$

respectively, which are the real and imaginary parts of R_k as defined in (9a) and (9b), respectively, where

$$R_{k,m}^c = \int_0^T c_k(t-\hat{\tau}_k)c_m(t-\hat{\tau}_m)\cos\left(2\pi\delta f_{k,m}^A t\right) dt \tag{31a}$$

$$R_{k,m}^s = \int_0^T c_k(t-\hat{\tau}_k)c_m(t-\hat{\tau}_m)\sin\left(2\pi\delta f_{k,m}^A t\right) dt. \tag{31b}$$

As a result, the expressions (30a) and (30b) build a system of linear equations with $2K$ variables, α_k^I and α_k^Q, and $2K$ measurements, R_k^I and R_k^Q, since $k = 1, 2, \ldots, K$. Defining

$$\underline{\alpha} \triangleq \left[\alpha_1^I, \alpha_2^I, \ldots, \alpha_K^I, \alpha_1^Q, \alpha_2^Q, \ldots, \alpha_K^Q\right]^T \tag{32a}$$

$$\mathbf{R}_A \triangleq \left[R_1^I, R_2^I, \ldots, R_K^I, R_1^Q, R_2^Q, \ldots, R_K^Q\right]^T \tag{32b}$$

$$\mathbf{R} \triangleq \begin{bmatrix} \mathbf{R}_c & \mathbf{R}_s \\ -\mathbf{R}_s & \mathbf{R}_c \end{bmatrix}, \tag{32c}$$

where

$$\mathbf{R}_c = \begin{bmatrix} R_{1,1}^c & R_{1,2}^c & \ldots & R_{1,K}^c \\ R_{2,1}^c & R_{2,2}^c & \ldots & R_{2,K}^c \\ \vdots & \vdots & \ddots & \vdots \\ R_{K,1}^c & R_{K,2}^c & \ldots & R_{K,K}^c \end{bmatrix} \tag{33a}$$

$$\mathbf{R}_s = \begin{bmatrix} R_{1,1}^s & R_{1,2}^s & \ldots & R_{1,K}^s \\ R_{2,1}^s & R_{2,2}^s & \ldots & R_{2,K}^s \\ \vdots & \vdots & \ddots & \vdots \\ R_{K,1}^s & R_{K,2}^s & \ldots & R_{K,K}^s \end{bmatrix}, \tag{33b}$$

and using the matrix inversion lemma [21], the algebraic solution for $\underline{\alpha}$ can be obtained as

$$\underline{\alpha} = \mathbf{R}^{-1}\mathbf{R}_A = \begin{bmatrix} \mathbf{U} & -\mathbf{VU} \\ \mathbf{VU} & \mathbf{U} \end{bmatrix} \mathbf{R}_A, \tag{34}$$

where

$$\mathbf{U} = \left(\mathbf{R}_c + \mathbf{R}_s\mathbf{R}_c^{-1}\mathbf{R}_s\right)^{-1} \tag{35a}$$

$$\mathbf{V} = \mathbf{R}_c^{-1}\mathbf{R}_s. \tag{35b}$$

Since computing (35a), (35b), and (34) requires $2K^3 + 2K^2$, K^2, and $6K^2$ complex multiplications, respectively, the total number of complex multiplications $2K^3 + 9K^2$ is much smaller than computing $\mathbf{R}^{-1}$ directly.

C. Fast Cross-Correlation Algorithm

The proposed fast computing algorithm for τ_k, f_D^k, and α_k in Sections III-A and III-B can reduce the computational complexity of the ML detection, however, there are still a large number of correlations required for the MSML estimation; there are $K(K-1)/2$ cross-correlations for L_{CC} (11) and α_k for every hypothesis of $\{\hat{\tau}_k, \hat{f}_D^k\}$, and K auto-correlations for L_{AC} (8) for each code phase and Doppler frequency hypothesis of the reference satellite m signal. Considering $2L_c$ $(= 2 \cdot 1023) \times N_{H_f}$ possible code phases and Doppler frequency ambiguities of the satellite m signal in A-GPS, the total number of correlations may be too high computational cost for a cheap A-GPS receiver.

From the analysis in Sections II and III-B, it is clear that most of computations in the MSML estimation is for the cross-correlations such as $R_{k,m}^c$ (31a) and $R_{k,m}^s$ (31b). To reduce the computational complexity for the massive cross-correlations, we propose a numerical approximation method for the cross-correlations using a set of pre-computed partial cross-correlation data that can be stored in the A-GPS receiver. Since the maximum relative Doppler frequency difference $\delta f_{k,m}^A$ between satellite m and satellite k is about 10 kHz (it can be only 5 kHz if the selected reference satellite m is at the zenith), $\cos(2\pi\delta f_{k,m}^A t)$ is varying very slowly relative to the $c_k(t-\hat{\tau}_k)c_m(t-\hat{\tau}_m)$ in the integrals (31a) and (31b). As a result, denoting $N_T = f_s T = N_c N_p N_q$ as the number of total samples during the correlation interval T for a sampling frequency $f_s = 1/T_s$, it is found that

$$R_{k,m}^c = \sum_{n=0}^{N_cN_q-1} \int_{\frac{nT}{N_cN_q}}^{\frac{(n+1)T}{N_cN_q}} c_k(t-\hat{\tau}_k) \times c_m(t-\hat{\tau}_m)\cos\left(2\pi\delta f_{k,m}^R t\right) dt \tag{36a}$$

$$\simeq \sum_{n=0}^{N_cN_q-1} \cos\left(\frac{(2n+1)\pi\delta f_{k,m}^A T}{N_cN_q}\right) \times \int_{\frac{nT}{N_cN_q}}^{\frac{(n+1)T}{N_cN_q}} c(t-\hat{\tau}_k)c(t-\hat{\tau}_m)\, dt \tag{36b}$$

$$\simeq \sum_{n=0}^{N_cN_q-1} \cos\left(\frac{(2n+1)\pi\delta f_{k,m}^A T}{N_cN_q}\right) R_{k,m}^p(n) \tag{36c}$$

$$R_{k,m}^s \simeq \sum_{n=0}^{N_cN_q-1} \sin\left(\frac{(2n+1)\pi\delta f_{k,m}^A T}{N_cN_q}\right) R_{k,m}^p(n), \tag{36d}$$

where

$$R_{k,m}^p(n) = \sum_{l=nN_p+1}^{(n+1)N_p} c_k[l-\hat{\tau}_k]c_m[l-\hat{\tau}_m] \tag{37}$$

is a partial cross-correlation between the segments of N_pT_s long partial PRN code samples $c_k(t-\hat{\tau}_k)$ and $c_m(t-\hat{\tau}_m)$, N_c is the number of code periods in T. Note that N_q should be large enough, but it can be sufficiently smaller than L_c so that $R_{k,m}^p(n)$ can be pre-computed and stored in a memory of the A-GPS receiver for all n $(= 0, 1, \ldots, N_q - 1)$, k, and m $(k, m \in \{1, 2, \ldots, K\})$. In practice, N_q should be multiple times larger than the maximum number of cycles of the cosine and sine terms in (36c) and (36d). Fig. 2 shows the approximation performance of (36c) and (36d) with respect to the true $R_{k,m}^c$ (31a) and $R_{k,m}^s$ (31b) obtained from 10^5 Monte Carlo simulations of arbitrary two GPS PRN codes between 1 and 30 with random code phases. The mean approximation error is zero as expected from (36c) and (36d) and is very small comparing to the true values of $R_{k,m}^c$ and $R_{k,m}^s$ so that the approximation error cannot make a noticeable contribution to L_{CC}. Note also that depending on the memory capacity of an A-GPS receiver, $R_{k,m}^c$ (31a) and $R_{k,m}^s$ (36c) can be pre-computed and stored for every relative Doppler frequency hypothesis between two satellites, which, for $T = 1$ ms, requires about 2×20 times larger memory than the memory required for $R_{k,m}^p(n)$ alone. Using the approximations in (36c) and (36d), approximation to L_{CC} (11) is derived as

$$L_{CC} \simeq \sum_{k=1}^{K}\sum_{m=1}^{K}\Bigg[\frac{\left(\alpha_k^I\alpha_m^I + \alpha_k^Q\alpha_m^Q\right)}{2} \times \sum_{n=0}^{N_cN_q-1}\cos\left(\frac{(2n+1)\pi\delta f_{k,m}^A T}{N_cN_q}\right)R_{k,m}^p(n) + \frac{\left(\alpha_k^I\alpha_m^Q - \alpha_k^Q\alpha_m^I\right)}{2} \times \sum_{n=0}^{N_cN_q-1}\sin\left(\frac{(2n+1)\pi\delta f_{k,m}^A T}{N_cN_q}\right)R_{k,m}^p(n)\Bigg]. \tag{38}$$

IV. Performance Analysis

In this section, we provide the theoretical performance analysis of the proposed fast MSML algorithm (i.e., the MSML estimation using the proposed three fast computation algorithms) in terms of SNR and computational complexity. In Section IV-A, SNR improvement and detection and false alarm

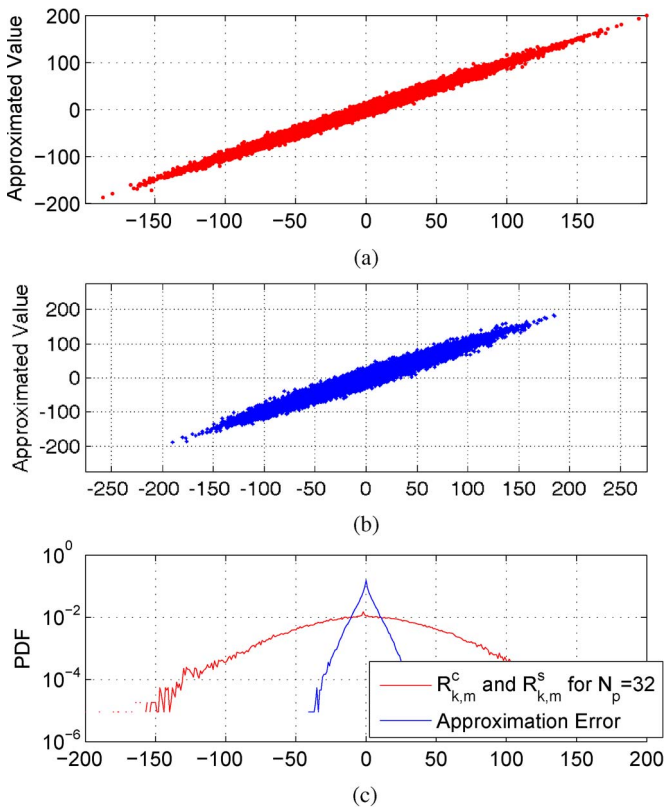

Fig. 2. Precision of the numerical approximation to $R^c_{k,m}$ and $R^s_{k,m}$. (a) $R^c_{k,m}$ (31a) and $R^s_{k,m}$ (31b) for $N_p = 16$; (b) $R^c_{k,m}$ (31a) and $R^s_{k,m}$ (31b) for $N_p = 32$; (c) PDFs of approximation errors, $R^c_{k,m}$, and $R^s_{k,m}$ for $N_p = 32$.

probabilities of the proposed algorithm are investigated, and in Section IV-B, the computational complexity is analyzed and compared with other techniques. For SNR and computational complexity, the conventional FFT-based search technique [11] and the non-coherent MS acquisition algorithm [17] that is a computationally more efficient algorithm than a number of MS and MSML algorithms introduced in the literature are used for the performance comparison, respectively.

A. Detection Performance

Since the proposed fast MSML algorithm removes the effect of ISI L_{CC} (38) on the auto-correlation output L_{AC} (8), the performance should be measured with the interference removed detection variable of the satellite k as

$$Z_1 = \left[\int_0^T \left[r(t) - \sum_{\substack{l=1\\ l\neq k}}^{K} s_l(t)\right] c_k^I \, dt\right]^2 + \left[\int_0^T \left[r(t) - \sum_{\substack{l=1\\ l\neq k}}^{K} s_l(t)\right] c_k^Q \, dt\right]^2, \quad (39)$$

and when c_k^I and c_k^Q are from the correct code phase and Doppler frequency hypothesis H_1 (i.e., $c_k^I|H_1$ and $c_k^Q|H_1$) the signal and noise powers in Z_1 are

$$S_1 = (T\alpha_k)^2 \quad (40a)$$

$$V_1 = TN_0, \quad (40b)$$

respectively. In discrete-time domain, T in (40a) and (40b) is replaced by N_T, and the signal-to-noise-ratio (SNR) of Z_1 becomes

$$\text{SNR}|_{Z_1} = \frac{N_T\alpha_k^2}{N_0}. \quad (41)$$

On the other hand, the decision variable of the conventional correlation technique is

$$Z_2 = \left(R_k^I\right)^2 + \left(R_k^Q\right)^2, \quad (42)$$

and the signal and noise powers of Z_2 for $c_k^I|H_1$ and $c_k^Q|H_1$ are

$$S_2 = (T\alpha_k)^2 \quad (43a)$$

$$V_2 = TN_0 + I_{K-1}, \quad (43b)$$

respectively, so that the signal-to-noise ratio of Z_2 is [8]

$$\text{SNR}|_{Z_2} = \frac{N_T^2\alpha_k^2}{N_TN_0 + I_{K-1}}. \quad (44)$$

The quantity I_{K-1} in (43b) represents the variance of zero-mean ISI between satellite k and other $K-1$ satellites such that

$$I_{K-1} = \left[\int_0^T c_k^I \sum_{\substack{l=1\\ l\neq k}}^{K} \left[\alpha_l^I c_l^I - \alpha_l^Q c_l^Q\right] dt\right]^2 + \left[\int_0^T c_k^Q \sum_{\substack{l=1\\ l\neq k}}^{K} \left[\alpha_l^I c_l^I - \alpha_l^Q c_l^Q\right] dt\right]^2 = V\left(c_k^I\right)^2 + V\left(c_k^Q\right)^2. \quad (45)$$

When there is no Doppler frequency difference between the satellite signals, the distribution of the variance I_{K-1} of the ISI may be approximated by a Gaussian distribution [23]. However, when there are unknown and non-negligible Doppler frequencies between the satellite signals, the variance I_{K-1} has a slightly narrower distribution than when there is no Doppler frequency [24]. When there is zero relative Doppler frequency between satellites k and l, rough estimates of $V(c_k^I)^2$ and $V(c_k^Q)^2$ can be found using Welch bounds [22] as

$$V\left(c_k^I\right)^2 = V\left(c_k^I\right)^2 \le \frac{N_T\Phi_{\max}^2}{2} E\left[\left(\sum_{\substack{l=1\\ l\neq k}}^{K} \alpha_l\right)^2\right], \quad (46)$$

where $\Phi_{\max}$ is the lower bound on the peak cross-correlation between an arbitrary pair of Gold sequences. However, there are non-zero relative Doppler frequency between satellites k and l, the cross-correlation between any two GPS satellite

signals shows about -60 dB ~ -21 dB (with mean about -35 dB) relative to the auto-correlation [24]. In other words, the cross-correlation amplitude between satellite k and l is about $0.001 \sim 0.0891$. Since the interference signals are mutually independent

$$V\left(c_k^I\right)^2 + V\left(c_k^I\right)^2 \approx N_T^2 \sum_{\substack{l=1 \\ l\neq k}}^{K} \beta_l^2 \alpha_l^2, \tag{47}$$

where $0.001 \leq \beta_l \leq 0.0891$, and the SNR of Z_2 can be expressed as

$$\text{SNR}|_{Z_2} \approx \frac{N_T \alpha_k^2}{N_0 + N_T \sum_{\substack{l=1 \\ l\neq k}}^{K} \beta_l^2 \alpha_l^2}. \tag{48}$$

In [25], it is indicated that the ISI of a satellite can be small when T/T_1 is large and the Doppler frequency difference is not close to an integer multiple of 1 kHz, which is the case for a small β_l. Note that both the signal energy and the ISI increase linearly with N_T. Therefore, when N_T increases, the ISI governs the SNR$|_{Z_2}$ so that the SNR$|_{Z_2}$ does not increase with N_T. In addition, when $\beta_l \alpha_l$ and N_T are large, detection of a weak target signal from satellite k is not easy as long as the interference is not removed sufficiently.

In the following, we investigate the performance of the proposed fast MSML algorithm for $TN_0 > I_{K-1}$ and $TN_0 < I_{K-1}$, which represent a situation with a strong target signal k and weak or moderate ISI and another situation with a weak target signal and large enough ISI to suppress the noise power, respectively. In fact, $TN_0 \approx I_{K-1}$ is only a special case when there is a 3 dB loss in the SNR due to the ISI. Therefore, we assume that $TN_0 > I_{K-1}$ and $TN_0 < I_{K-1}$ represent most of the channel conditions in practice. As a result, it can be found that both Z_1 (39) and Z_2 (42) can be approximated by a non-central χ^2 distribution with 2 degrees of freedom for $c_k^I|H_1$ and $c_k^Q|H_1$ as

$$P_1(Z_i) = \frac{1}{V_i} \exp\left(-\frac{Z_i + S_i^2}{V_i}\right) I_0\left(\frac{2S_i\sqrt{Z_i}}{V_i}\right), \tag{49}$$

or a central χ^2 distribution with 2 degrees of freedom for $c_k^I|H_0$ and $c_k^Q|H_0$ as

$$P_0(Z_i) = \frac{1}{V_i} \exp\left(\frac{-Z_i}{V_i}\right) \tag{50}$$

where $i = 1, 2$ and $I_0(\cdot)$ is the zeroth order modified Bessel function of the first kind, and H_1 and H_0 represent the correct hypothesis and incorrect hypothesis in the two-dimensional search space, respectively. The detection, miss, and false alarm probabilities are readily available from the literature [8] and [19]

$$P_D = \int_{\gamma_i}^{\infty} P_1(x)\, dx = \int_{\gamma_i/V_i}^{\infty} e^{-x+\mu_i} I_0(2\sqrt{\mu_i x})\, dx$$

$$= Q\left(S_i\sqrt{\frac{2}{V_i}}, \sqrt{\frac{2\gamma_i}{V_i}}\right) \tag{51a}$$

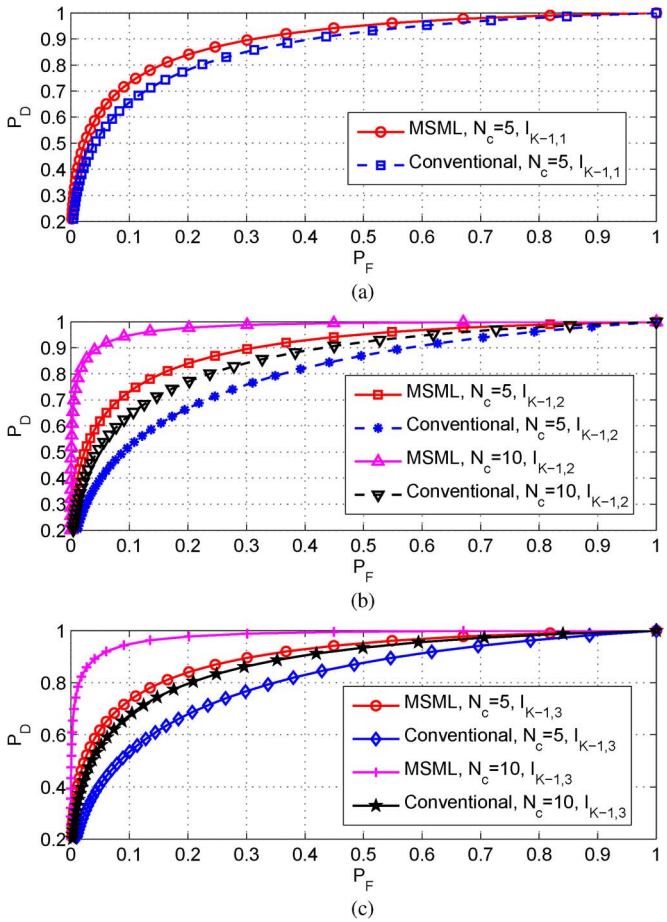

Fig. 3. ROC improvement with the proposed fast MSML algorithm. (a) Scenario 1; (b) Scenario 2; (c) Scenario 3.

$$P_M = 1 - P_D \tag{51b}$$

$$P_F = \int_{\gamma_i}^{\infty} P_0(x)dx = \exp\left(-\frac{\gamma_i}{V_i}\right) \tag{51c}$$

respectively, where $\mu_i = S_i^2/V_i$, γ_i is the detection threshold for Z_i $(i = 1, 2)$, and $Q(a, b)$ is the Marcum's Q-function [26].

In fact, when the ISI is not removed in the MSML estimation (4c), the SNR of the proposed fast MSML algorithm can be found as (44), whereas the SNR can be as high as (41) when the ISI is sufficiently removed. The reduction of ISI results in a narrower distribution of $P_1(x)$, which leads to an increase of P_D (51a) when γ_i is smaller than the mean of the $P_1(x)$. On the other hand, due to the ISI reduction, V_i becomes smaller, and, thus, P_F (51c) becomes smaller. Therefore, the reduction of ISI increases the receiver operating characteristics (ROC) performance as shown in Fig. 3.

B. Complexity Issue

In this subsection, we analyze the computational complexity of the proposed fast MSML algorithm. For simplicity of algebraic analysis, it is assumed that the reference satellite m is near the zenith (i.e., $E_m \simeq 90°$), and that the elevation angles E_k and azimuth angles A_k of $K-1$ satellites are uniformly distributed

over [0°, 90°) and [0, 360°), respectively. The assumption may not represent a general situation, but is sufficient to develop a rough estimate of the complexity required for the proposed fast MSML algorithm. In addition, the coverage area C of a node-B is assumed to be a flat circular area with radius R.

The proposed fast MSML algorithm may perform auto-correlations in the frequency domain using FFT to compute R_k^I (9a) and R_k^Q (9b) for all $k \in \{1, 2, \ldots, K\}$ and estimate L_{AC}. Letting N_T be the number of FFT points, computing R_k^I and R_k^Q requires total N_T-point FFT for $K+1$ times (including FFT of the incoming signal), KN_T complex multiplications in the frequency domain, and K times N_T-point IFFT, so that for a given Doppler frequency hypothesis the number of complex multiplications required for L_{AC} is

$$N_{AC} = (2K+1)N_T \log_2(N_T) + KN_T. \tag{52}$$

On the other hand, for a given set of K code phases and K Doppler frequencies of the K satellites, there are $K(K-1)/2$ cross-correlations for $R_{k,m}^c$ and $R_{k,m}^s$, N_cN_q multiplications for the approximations in (36c) and (36d), and $N_{H_c}(k)$ code phase hypothesis to test for each satellite. Let the location hypothesis $H_L(x, y)$ represent a small horizontal area of $\Delta r^2 \mathrm{m}^2$ over which K code phases and K Doppler frequencies of K satellites can be assumed constants. Since $f_s = 2R_c$ and $\Delta t = 0.5T_c$, a satellite k at elevation angle E_k can have a code phase change larger than $0.5T_c$ at every $c\Delta t/\cos(E_k) = 0.5cT_c/\cos(E_k)$ (=150 m for GPS C/A code signal from 0° elevation angle) within C along the direction to the azimuth angles A_k and $-A_k$, whereas there is no code phase change within C along the direction perpendicular to the azimuth angles A_k and $-A_k$. In addition, as the elevation angle E_k increases, $c\Delta t/\cos(E_k)$ increases. Therefore, the minimum distance between two points within C for a code phase change about $0.5T_c$ is $c\Delta t/\cos(E_k) = 0.5cT_c/\cos(E_k) \geq 0.5cT_c$, so that $\Delta r \leq 150/\sqrt{2} \approx 100$ m can be a sufficient condition to detect the code phase of the incoming signal in $0.5T_c$ resolution. As a result, the total number of complex multiplications for L_{CC} is

$$N_{CC} < \frac{\pi R^2 K(K-1)N_cN_q}{2\Delta r^2} \tag{53}$$

for all location hypotheses $H_L(x, y)$ in C. Note that N_{CC} in (53) is obviously N_p times smaller than the number of complex multiplications for all cross-correlations. In addition, since computing U (35a) and V (35b) require $2K^3 + 3K^2$ multiplications, obtaining R^{-1} (34) requires $2K^3 + 5K^2$ multiplications so that there are

$$N_{IV} \leq \frac{\pi R^2(2K^3 + 9K^2)}{\Delta r^2} \tag{54}$$

multiplications to find $\underline{\alpha}$ for all location hypotheses $H_L(x, y)$ in C. Note that the inequalities in (53) and (54) are from the fact that the K code phases for a location hypothesis $H_L(x, y)$ are not completely different from the K code phases of the neighboring location hypothesis $H_L(x \pm \Delta r, y \pm \Delta r)$, so that the number of new code phases to test for a location hypothesis is less than K. Considering N_{H_f} Doppler frequencies, the total number of multiplications for the proposed fast MSML algorithm is

$$N_{all} = N_{H_f}(N_{AC} + N_{IV}) + N_{CC}, \tag{55}$$

since N_{AC} and N_{IV} require R_k^I (9a) and R_k^Q (9b) for each Doppler frequency hypothesis. Assuming $K = 8$, $N_c = 1$, $N_T = 2N_cL_c$ (i.e., $f_s = 2R_c$), $N_q = 128$, $\Delta r = 100$ m, $R = 2$ Km, and $N_{H_f} = 3$, for an example, $N_{all} < 3(4 \times 10^5 + 2 \times 10^6) + 4.5 \times 10^6 \simeq 1.2 \times 10^7$. When $N_c = 5$ (i.e., $T = 5$ ms) in the above example, $N_{all} < 3(2.4 \times 10^6 + 2 \times 10^6) + 2.3 \times 10^7 \simeq 3.6 \times 10^7$, which can take less than a second for a modern processor capable of GHz computing speed. Comparing to the conventional FFT-based search in standalone GPS receivers for $T = 1$ and 5, where $D_f = 21$, and 105 Doppler frequency hypotheses are tested (assuming $\Delta f_m = 1/(2T)$), respectively, $N_{all}|_{\text{conventional}} = D_f N_{AC} \simeq 8.4 \times 10^6$ and 2.5×10^8, respectively. In addition, when compared to A-GPS receivers using the conventional FFT-based search and utilizing the proposed reduced search technique $N_{H_f} = 3$, it becomes $N_{all}|_{\text{A-GPS}} = N_{H_f}N_{AC} \simeq 1.2 \times 10^6$ and 7.2×10^6, respectively. Therefore, the proposed fast MSML algorithm requires much smaller computations than the conventional FFT-based standalone GPS search technique, but may require about 5 to 10 times more computations than an FFT-based A-GPS search technique. In the non-coherent MS acquisition technique [17], when the GPS receiver uses assistance from an asynchronous cellular network and FFT-based signal search with $T = 1$ ms, the number of complex multiplications is about $N_{H_f}N_{AC}$ (neglecting the squaring process) which maybe a smaller number of complex multiplications than the proposed fast MSML algorithm.

In addition to the receiver computing power for multiplications, the proposed fast MSML algorithm requires pre-computed and stored $R_{k,m}^p$, for $k, m \in \{1, 2, \ldots, K\}$. Since the size of $R_{k,m}^p$ is $N_q(= N_T/(N_cN_p))$ and there are K satellites, the memory size required to store $R_{k,m}^p$ is

$$M_R = \frac{K(K-1)}{2} N_qN_b, \tag{56}$$

where N_b is the number of bits to express each element of $R_{k,m}^p$. Since each element of $R_{k,m}^p$ is an inner product between the partial segments (with length $N_p \gg 1$) of two different PRN codes, $R_{k,m}^p \ll N_p$ when N_p is large. Assuming $|R_{k,m}^p| \leq 16$ for $N_p = 16$ (i.e., $N_q = 128$) and $K = 30$ (for all GPS satellites), $N_b = 4$ bytes and $M_R \simeq 0.2$ Mbyte, which is not a heavy data size to store for modern portable devices.

V. Numerical Simulations

In this section, we compare the ROC and SNR improvement with the proposed fast MSML algorithm to those of conventional techniques. To compare the ROC and detection probability, we compare the proposed fast MSML algorithm with the conventional FFT-based search technique, and for the SNR of a detected satellite signal coherent MSML algorithm [15], coherent MS acquisition technique [16], and non-coherent MS acquisition technique [17] are compared. In the following

TABLE I
C/N_0 OF SATELLITE SIGNALS FOR FIG. 3

Satellite num.	1	2	3	$4 \sim 8$
scenario 1	28	38	38	38
scenario 2	28	48	48	38
scenario 3	28	[35,48]	[35,48]	[35,48]

simulations, it is assumed that $K = 8$, $N_0 = -205$ dBW/Hz, and the receiver has a sampling rate $f_s = 2R_c$, pre-correlation bandwidth $B = 2.046$ MHz, $N_q = 128$, $\Delta r = 100$ m, $R = 2$ Km, and correlation length $T = N_c$ ms $(= N_T T_s)$.

In Fig. 3, numerical evaluation of the ROC with SNR in (41) and (48) are compared for three scenarios, where a receiver is trying to acquire a weak target GPS $L1$ frequency C/A code signal (i.e., C/N_0 is only 28 dB-Hz) with $N_c = 5$ and $N_c = 10$ under a heavy ISI from $K - 1$ other satellites. The first scenario represents environments where the strengths of the $K - 1$ satellite signals are moderate (i.e., C/N_0s are about 38 dB-Hz). The second scenario is when there are two strong signals (i.e., C/$N_0 = 48$ dB-Hz) and $K - 3$ moderate signals, which represents situations when the A-GPS receiver is near a window inside a building or in urban canyon. The third scenario represents general environments, where the C/N_0s of $K - 1$ interfering satellites are random and uniformly distributed in [35, 48] dB-Hz. In all three scenarios, β_l^2 in (47) is ideally assumed to have random and uniform distribution within $[-60, -21]$ dB for all $l \in \{1, 2, \ldots, K-1\}$ (48). The three scenarios are summarized in Table I. In Fig. 3, $I_{K-1,1}$, $I_{K-1,2}$, and $I_{K-1,3}$ denote the total ISI in the first, second, and third scenarios, respectively. Notice that the plots for MSML with $[N_c = 5, I_{K-1,1}]$, $[N_c = 5, I_{K-1,2}]$, and $[N_c = 5, I_{K-1,3}]$ show the same performance, and that MSML with $[N_c = 10, I_{K-1,2}]$ and $[N_c = 10, I_{K-1,3}]$ have the same ROC as well, since the ISI is canceled and only the noise and the target signal define the SNR (41). It is interesting to observe that conventional techniques with $[N_c = 5, I_{K-1,1}]$, $[N_c = 10, I_{K-1,2}]$, and $[N_c = 10, I_{K-1,3}]$ have similar ROC, because there is a strong ISI from strong satellite signals. Comparing the plots in Fig. 3, the proposed fast MSML algorithm can provide higher ROC improvement for larger N_c, which is expected from (44), since the effect of interference grows with the correlation length $T = 2N_c L_c$, while the effect of noise has an opposite tendency.

The benefit of the proposed fast MSML algorithm is the improved detection performance for weak signals. To demonstrate the advantage over the conventional parallel correlators, 10^5 Monte Carlo simulations of $K(= 8)$ GPS (C/A code) signal acquisitions are performed for three signal environments; the C/N_0's of K satellite signals are [28:1.5:38.5] dB-Hz (Environments-I), [38:1.5:48.5] dB-Hz (Environments-II), and [28, 29, 36:1:38, 46:1:48] dB-Hz (Environments-III), which represent weak signal environments, strong signal environments, mixed signal environments, respectively, where $[a : b : c] = [a, a + b, a + 2b, \ldots, a + \lfloor (c - a)/b \rfloor b]$. The C/$N_0$s of the K satellites are summarized in Table II. The simulation results are analyzed to obtain the SNR and probability of detection in the three environments. In Figs. 4(a)–6(a), the coherent SNR (i.e., the SNR measured with the correlation output before the root-sum-of-squares (RSS) operation) [18] is measured for the

TABLE II
C/N_0 OF SATELLITE SIGNALS FOR FIGS. 4–6

Satellite num.	1	2	3	4	5	6	7	8
Environments-I	28	29	31	32.5	34	35.5	37	38.5
Environments-II	38	39.5	41	42.5	44	45.5	47	48.5
Environments-III	28	29	36	37	38	46	47	48

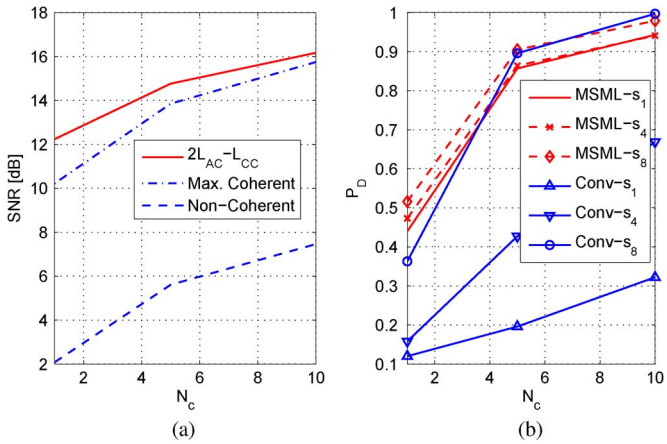

Fig. 4. Performance of the proposed fast MSML algorithm: Environments-I. (a) SNR comparison; (b) Probability of detection.

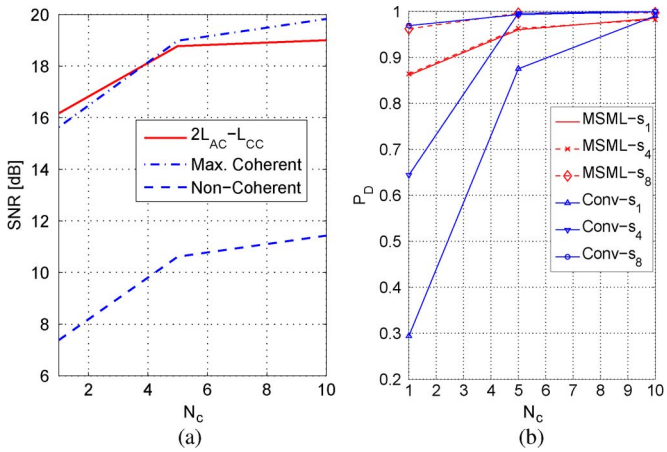

Fig. 5. Performance of the proposed fast MSML algorithm: Environments-II. (a) SNR comparison; (b) Probability of detection.

proposed detection variable $2L_{AC} - L_{CC}$, a detection variable built by the coherent sum of K auto-correlation results when the carrier phases ϕ_k $(k = 1, 2, \ldots, K)$ are perfectly compensated (denoted as Max. Coherent in the figures) and a detection variable built by the non-coherent sum of K auto-correlation results (denoted as Non-Coherent in the figures). Therefore, it can be found that the SNR of Max. Coherent and the SNR of Non-Coherent are the maximum achievable SNRs for coherent MS acquisition technique [16] and the non-coherent MS acquisition technique [17], respectively. In addition, it should be noticed that the proposed fast MSML algorithm has a slightly lower performance than the MSML algorithm in [15], since the proposed algorithm has a Doppler frequency search step size of $1/(2T)$ which is much smaller than 10 Hz used in [15]. The results in Figs. 4(a)–6(a) demonstrate that the SNR of the proposed fast MSML algorithm often becomes higher than the SNR of Max. Coherent, which is possible because

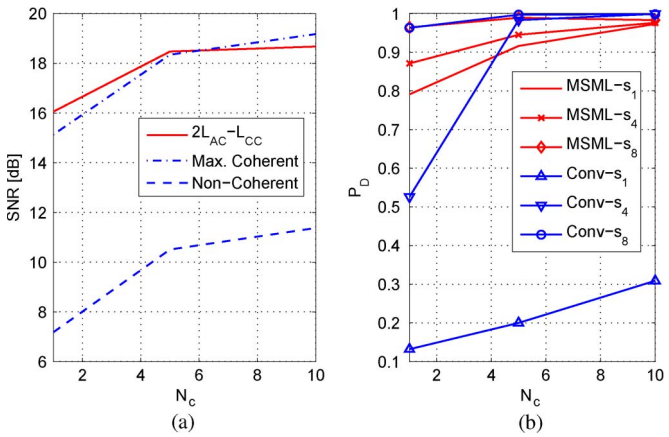

Fig. 6. Performance of the proposed fast MSML algorithm: Environments-III. (a) SNR comparison; (b) Probability of detection.

of the interference cancelation. In Figs. 4(b)–6(b), the probabilities of detection P_D of satellite 1, 4, and 8 (i.e., s_1, s_4, and s_8, respectively) are shown for the proposed fast MSML algorithm and the conventional correlator-based technique that obtains the auto-correlation output of each satellite signal separately. Note that the C/N$_0$'s of the three satellite signals are [28, 32.5, 38.5] dB-Hz, [38, 42.5, 48.5] dB-Hz, and [28, 37, 48] dB-Hz for Environments-I, Environments-II, and Environments-III, respectively. As shown, in most environments, the proposed fast MSML algorithm has a high probability of detection P_D even for weak satellite signals, and the P_D of weak signals with the proposed fast MSML algorithm is similar to the P_D of the strong satellite signals with the conventional correlator-based technique. In fact, this is because the proposed fast MSML algorithm detects K satellite signals all together. However, the detection failure of weak satellite signals occur when all of the strong satellite signals have the same code phase delays τ_k at multiple location hypothesis $H_L(x, y)$ within C. As shown in the simulation results, SNR improvement is the largest for the satellite 1 (the weakest satellite). It is because the interference by the other satellites (from 2 to 8) are the biggest to the satellite 1, whereas the interference to the satellite 8 is smallest and the SNR improvement is the lowest as expected.

It should be noted that the effect of the number of quantization bits B_q is not considered in the simulations, but $B_q \geq 2$ is good enough as many commercial GPS receivers using $B_q = 2$ can detect strong and weak signals with correlators.

VI. Conclusion

Three fast computing algorithms that significantly reduces computational complexity of multi-satellite maximum likelihood (MSML) estimation have been proposed for A-GPS receivers in asynchronous cellular networks. The performance of the proposed algorithm has been tested with numerous Monte Carlo simulations for GPS L1 C/A code signals. The simulations have shown that the proposed algorithm can have a large increase of the detection probability for weak signals buried under strong GPS signals and noise, which is not easy with the conventional correlator-based acquisition techniques. In addition, it has been shown that the proposed algorithm has lower computational complexity or better performance than the existing non-coherent MS acquisition technique, coherent MS technique, and MSML computation algorithm. As expected, it has been demonstrated that the performance of the proposed algorithm becomes better in weak signal detection when detected signals are stronger.

Appendix

To prove that the difference between (36a) and (36b) is approximately zero, we define $A^c_{k,m}$ as

$$A^c_{k,m} = \sum_{n=0}^{N_cN_q-1} \int_{\frac{n}{N_{cq}}}^{\frac{(n+1)}{N_{cq}}} c_k(t-\hat{\tau}_k)c_m(t-\hat{\tau}_m) \times \left[\cos\left(2\pi\delta f^A_{k,m}t\right) - \cos\left(\frac{(2n+1)\pi\delta f^A_{k,m}}{N_{cq}}\right)\right] dt, \quad (57)$$

where $N_{cq} = N_cN_q/T$. Then, the integration term of (57) is,

$$\int_{\frac{n}{N_{cq}}}^{\frac{(n+1)}{N_{cq}}} F_a(t)q_a(t)dt = F_a(t)Q_a(t)\Big|_{\frac{n}{N_{cq}}}^{\frac{(n+1)}{N_{cq}}} - \int_{\frac{n}{N_{cq}}}^{\frac{(n+1)}{N_{cq}}} f_a(t)Q_a(t)\,dt \quad (58)$$

where

$$F_a(t) = c_k(t-\hat{\tau}_k)c_m(t-\hat{\tau}_m) \quad (59a)$$

$$q_a(t) = \cos\left(2\pi\delta f^A_{k,m}t\right) - \cos\left(\frac{(2n+1)\pi\delta f^A_{k,m}}{N_{cq}}\right) \quad (59b)$$

$$f_a(t) = \frac{d}{dt}\left(F_a(t)\right) \quad (59c)$$

$$Q_a(t) = \int q_a(t)\,dt. \quad (59d)$$

Therefore,

$$Q_a(t) = \left[\frac{\sin\left(2\pi\delta f^A_{k,m}t\right)}{2\pi\delta f^A_{k,m}} - \cos\left(\frac{(2n+1)\pi\delta f^A_{k,m}}{N_{cq}}\right)\right]_{\frac{n}{N_{cq}}}^{\frac{(n+1)}{N_{cq}}} \quad (60a)$$

$$= \cos\left(\frac{(2n+1)\pi\delta f^A_{k,m}}{N_{cq}}\right)\frac{1}{N_{cq}}\left(\frac{\sin\left(\frac{\pi\delta f^A_{k,m}}{N_{cq}}\right)}{\frac{\pi\delta f^A_{k,m}}{N_{cq}}} - 1\right). \quad (60b)$$

In (60b), when $(\delta f^A_{k,m})/N_{cq} \ll 1$, $Q_a(t) \simeq 0$, and $A^c_{k,m} \simeq 0$.

References

[1] *Position Determination Service Standards for Dual-Mode Spread Spectrum Systems—Addendum*, TIA/EIA IS-801-1, Mar. 2001.

[2] *Stage 2 functional specification of UE positioning in UTRAN*, 3GPP TS 25.305 V4.7.0, Dec. 2003.

[3] *Radio Subsystem Synchronization (Release 8)*, 3GPP TS 45.010 V8.0.0, May 2008.
[4] *User Equipment (UE) Radio Transmission and Reception (FDD) (Release 8)*, 3GPP TS 25.101 V8.0.0, Sep. 2007.
[5] *Physical Layer Aspects for Evolved UTRA (Release 7)*, 3GPP TR 25.814 V1.0.1, Nov. 2005.
[6] S.-H. Kong and W. Nam, "A-GNSS sensitivity for parallel acquisition in asynchronous cellular networks," *IEEE Trans. Wireless Commun.*, vol. 9, no. 12, pp. 3770–3778, Dec. 2010.
[7] E. Souour and S. C. Gupta, "Direct-sequence spread-spectrum parallel acquisition in a fading mobile channels," *IEEE Trans. Commun.*, vol. 38, no. 7, pp. 992–998, Jul. 1990.
[8] A. J. Viterbi, *CDMA: Principles of Spread Spectrum Communication*. Reading, MA, USA: Addison-Wesley, 1995.
[9] B. Kim and S.-H. Kong, "Two dimensional compressed correlator for fast acquisition in GNSS," in *Proc. ION ITM*, San Diego, CA, USA, Jan. 2013, pp. 519–525.
[10] Y. Jiang, Z. Shufang, H. Qing, and S. Xiaowen, "A new FFT-based acquisition algorithm for GPS signals," in *Proc. Int. Workshop ETT/Int. Workshop GRS*, 2008, vol. 2, pp. 415–419.
[11] D. Akopian, "Fast FFT based GPS satellite acquisition methods," *Proc. Inst. Elect. Eng.—Radar Sonar Navig.*, vol. 152, no. 4, pp. 277–286, Aug. 2005.
[12] K. Borre, D. Akos, N. Bertelsen, P. Rinder, and S. Jensen, *A Software Defined GPS and Galileo Receiver: A Single Frequency Approach*. Cambridge, MA, USA: Birkhaüser, 2007.
[13] C. Yang, J. Vasquez, and J. Chaffee, "Fast direct P(Y)-code acquisition using XFAST," in *Proc. ION GPS*, Sep. 1999, pp. 317–324.
[14] H. Li, X. Cui, M. Lu, and Z. Feng, "Dual-folding based rapid search method for long PN-code acquisition," *IEEE Trans. Wireless Commun.*, vol. 7, no. 12, pp. 5286–5296, Dec. 2008.
[15] I. F. Progri, M. C. Bromberg, and W. R. Michalson, "An enhanced acquisition process of a maximum likelihood GPS receiver," in *Proc. ION NTM*, San Diego, CA, USA, Jan. 2004, pp. 390–398.
[16] R. DiEsposti, "GPS PRN code signal processing and receiver design for simultaneous all-in-view coherent signal acquisition and navigation solution determination," in *Proc. ION NTM*, San Diego, CA, USA, Jan. 2007, pp. 91–103.
[17] P. Axelrad, J. Donna, and M. Mitchell, "Enhancing GNSS acquisition by combining signals from multiple channels and satellites," in *Proc. ION GNSS*, Savannah, GA, USA, Sep. 2009, pp. 2617–2628.
[18] F. V. Diggelen, *A-GPS: Assisted GPS, GNSS, and SBAS*. Norwood, MA, USA: Artech House, 2009.
[19] E. D. Kaplan and C. J. Hegarty, *Understanding GPS: Principles and Applications*, 2nd ed. Norwood, MA, USA: Artech House, 2006.
[20] S.-H. Kong, "Statistical analysis of urban GPS multipaths and pseudo-range measurement errors," *IEEE Trans. Aerosp. Electron. Syst.*, vol. 47, no. 2, pp. 1101–1113, Apr. 2011.
[21] M. H. Hayes, *Statistical Digital Signal Processing and Modeling*. Hoboken, NJ, USA: Wiley, 1996.
[22] L. R. Welch, "Lower bounds on the maximum cross-correlation of signals," *IEEE Trans. Inf. Theory*, vol. IT-20, no. 3, pp. 397–399, May 1974.
[23] H. Inaltekin, "Gaussian approximation for the wireless multi-access interference distribution," *IEEE Trans. Signal Process.*, vol. 60, no. 11, pp. 6114–6120, Nov. 2012.
[24] S. U. Qaisar and A. G. Dempster, "An analysis of L1-C/A cross correlation and acquisition effort in weak signal environments," presented at the International Global Navigation Satellite Systems Society Symposium, Sydney, N.S.W., Australia, Dec. 4–6, 2007, Paper 107.
[25] Y. T. J. Morton *et al.*, "Assessment and handling of CA code self-interference during weak GPS signal acquisition," in *Proc. ION GPS/GNSS*, Portland, OR, USA, Sep. 2003, pp. 646–653.
[26] J. I. Marcum, "A table of Q-functions," Rand Corp., Santa Monica, CA, USA, Rep. RM-339, Jan. 1950.

Seung-Hyun Kong (M'06) received the B.S.E.E. degree from Sogang University, Seoul, Korea, in 1992, the M.S.E.E. degree from the Polytechnic University, Brooklyn, NY, USA, in 1994, and the Ph.D. degree in aeronautics and astronautics from Stanford University, Stanford, CA, USA, in 2006.

From 1997 to 2004, he was with Samsung Electronics Inc. and Nexpilot Inc., both in Korea, where his research focus was on 2G CDMA and 3G UMTS PHY and mobile positioning technologies. In 2006, he was involved with hybrid positioning technology development using wireless location signature and Assisted GNSS at Polaris Wireless, Inc. From 2007 to 2009, he was a member of the Research Staff at the Corp. R&D, Qualcomm Inc., San Diego, CA, USA, where his R&D focus was on indoor location technologies and advanced GNSS technologies. Since 2010, he has been an Assistant Professor with the CCS Graduate School for Green Transportation, Korea Advanced Institute of Science and Technology, Daejeon, Korea. His research interests include super-resolution signal processing, detection and estimation in navigation systems, and vehicular communication systems.